RTSIM: A COMPUTER MODEL OF REAL-TIME RADIOGRAPHY

T. Jensen, and J.N. Gray
Center for Nondestructive Evaluation
Iowa State University
Ames, IA 50011

INTRODUCTION

Real-time X-ray inspection is replacing film radiography in more and more applications. The rapid feedback provided by such systems greatly enhances throughput, especially in the case of complex objects requiring multiple views for complete inspection. When these systems are combined with powerful computing techniques, rapid image capture and enhancement and storage is possible. The productivity of these techniques would be increased with the ability to predict the sensitivity of a particular inspection without having to set up the equipment. Computer modeling of the inspection procedures can provide such information.

We have previously reported our work on a model of X-ray film radiography which we call XRSIM[1-4]. In our present work we have used this model as the basis for simulation of images produced by a real-time inspection system. In this paper we describe the parameters used in the model, and discuss some examples of the use of this simulation program, which we call RTSIM.

MODEL DESCRIPTION

A schematic overview of the real-time simulation model is shown in Fig. 1. The simulation of the X-ray generator and the interaction of X-rays in different materials follows directly from our previous work on XRSIM[1-4]. Ray paths are traced from the generator through the sample to an imaging plane which has been divided into an array of pixels. All geometric information needed to describe the sample comes from a standard CAD output file. Currently the interface to RTSIM accepts output from several CAD programs, with extension to other formats being straight forward. Also, as indicated, a simulated ellipsoidal flaw of arbitrary size and orientation can be placed anywhere within the object.

Figure 2 shows the basic features of a real-time imaging system which should be accounted for in a model. A typical image intensifier[5] is constructed from an evacuated tube whose front face consists of a scintillation screen to convert incident X-rays to light. This light, in turn, strikes a photocathode where it is converted to electrons which are

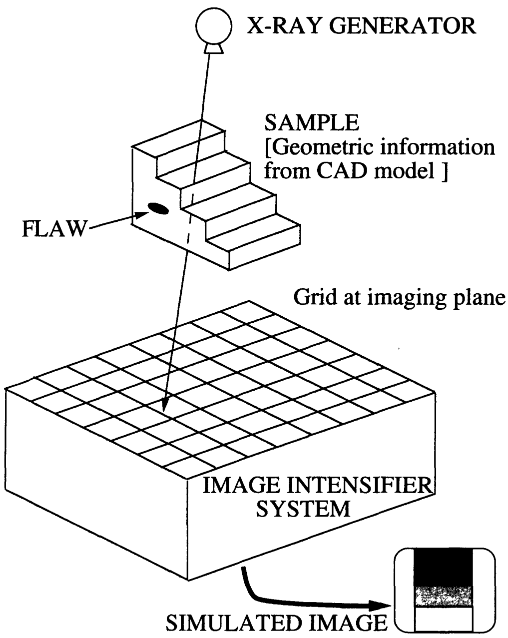

Fig. 1. Schematic overview of the RTSIM computer model.

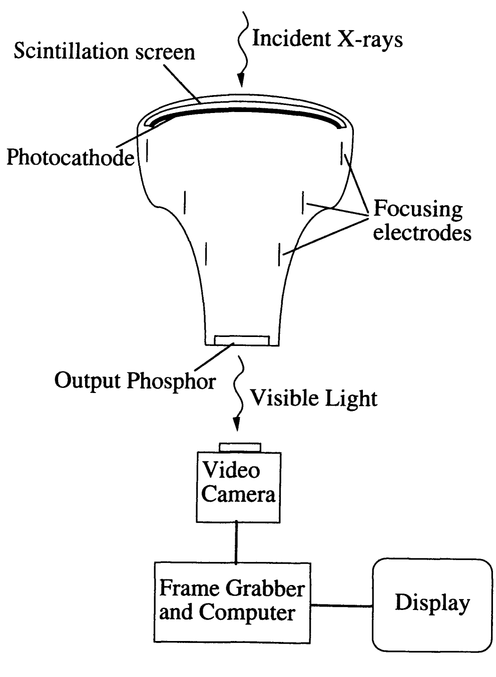

Fig. 2. Schematic representation of a typical real-time imaging system.

accelerated and focused onto an output phosphor screen where they are converted to visible light. This output screen is typically viewed by a video camera and the resulting image is captured for display and analysis.

We have developed our model to be general enough that a variety of systems can be simulated and compared. The computer program is driven by a set of parameter files which can easily be interchanged to represent different system configurations. The work presented here is based on a system assembled from the following components: an IRT model IXRS 320/3200 generator, a Toshiba six inch image intensifier tube, a Cohu model 4810 CCD camera with 640 x 480 pixels and 8-bit digitization, and a Data Translation model DT-2867 frame grabber.

A preliminary model of the image intensifier response has previously been reported on[6]. The results presented here extend this work. The basic elements that we will use to judge the accuracy of our model include: matching of greyscale values, spatial resolution, contrast sensitivity, and any geometric distortion.

One factor affecting spatial resolution is determined by the geometry of the camera and image intensifier coupling. This is easily modeled by accounting for the CCD pixel dimensions as well as the focal length of the camera lens and the lens-phosphor and lens-CCD distances. For typical cameras and a field of view 10 cm diameter or more, these geometric conditions will limit resolution to a few lp/mm. An intrinsic limit to the resolution is due to a phenomena called phosphor bloom. At both the input conversion screen and the output phosphor screen the generated light spreads radially a finite distance to blur the position of the incident X-ray. For the Toshiba tube the extent of blurring has been determined from an image of a sharp edge projected by a lead plate[6]. The measured data is well represented by a Gaussian blurring function.

One drawback in using image intensifier systems is the distortions that are introduced to images. It is difficult to maintain uniform electric fields over such large distances, and as a result, the amplification factor can vary over the face of the tube. In viewing a uniform radiation field with the six inch Toshiba tube we observed 40% higher response at the center of the tube than at the edges[7]. In our model this response is approximated by a quadratic dependence of the brightness on the distance from the center of the tube.

Another significant distortion is due to the fact that the input conversion screen is curved, whereas the output phosphor is flat. This results in a pincushion distortion, where straight lines near the edge of an image will appear to be curved. By imaging a uniform grid we have parameterized a transformation between the true coordinate system and the coordinate system of the distorted image as follows:

$$x_d = \sum_{m=0}^{3}\sum_{n=0}^{3} A_x(m,n) x_c^m y_c^n, \quad y_d = \sum_{m=0}^{3}\sum_{n=0}^{3} A_y(m,n) x_c^m y_c^n, \qquad (1)$$

where x_d and y_d are the distorted coordinates and x_c and y_c are the true coordinates. A_x and A_y are matrices of coefficients up to third order in the coordinates.

Contrast sensitivity will be related to the integration time and digitization accuracy of the camera. Eight-bit digitization is fairly common and 12-bit cameras are becoming more affordable. Any desired level of digitization accuracy can be simulated in the model. The standard TV read-out rate of 30 frames per second is very common in real-time systems, although a wide range of read-out rates are possible, and multiple frames can be averaged to improve contrast. The model also allows parameters corresponding to read-out rate and frame averaging to be adjusted.

Another important factor affecting the contrast sensitivity is the scale factor for relating incident X-ray flux to image greyscale value. There are many intermediate stages which can affect this value, and a complete model of all of the physical processes would be very time consuming. We have opted for a relatively simple empirical model in which we relate the greyscale level to the incident X-ray flux measured in Roentgens. A NaI(Tl) detector with a 600 μm diameter collimator was used to measure the X-ray flux.

In our earlier work[6] we found that the relation between incident flux and greyscale level depended on the voltage setting of the generator. Thus, it is expected that not only the total flux, but also the energy spectrum of the radiation incident on the imaging tube will determine the resulting greyscale value. The effect will be different for different materials and thicknesses. An example of this relationship is shown in Fig. 3a for a piece of aluminum 5 mm thick. Similar curves were acquired for aluminum thicknesses up to 35 mm. It is postulated that a relatively simple formula can be obtained by correlating the slope of the curves in Fig. 3a with the average energy of the X-rays incident at the face of the image intensifier. This information is plotted in Fig. 3b for several thicknesses of aluminum. Data for the thinner materials appears to follow a simple linear trend, whereas the trend is not so clear for the thicker materials.

It was subsequently realized that there is a discrepancy between the flux we measure using the NaI detector and the flux that is seen by the image intensifier. The NaI detector has a relatively small collimated active area which excludes most X-rays that have scattered in the sample, whereas the image intensifier is open to most scattered X-rays. Furthermore, the fraction of scattered X-rays increases as the sample thickness increases. In a simple test we observed that the curve for 23 mm thick aluminum fell much closer to the results for thinner samples when we masked off all but a small area of the image intensifier. It is evident that future improvements to the model will require a much more careful treatment of scattering. In the present version we have extrapolated the results from the thinner materials where scattering is minimal.

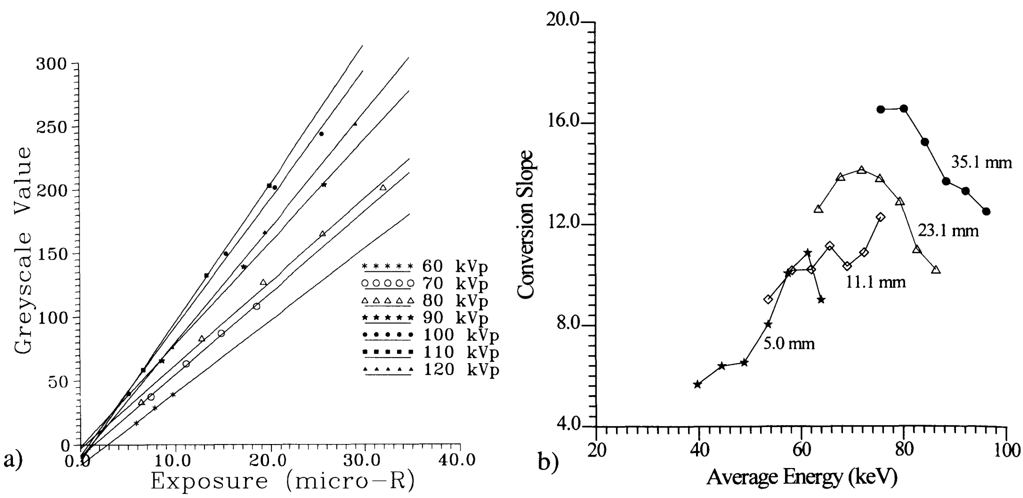

Fig. 3. a) Observed relation between greyscale value and exposure for transmission through 5.0 mm aluminum at different voltage settings. b) Correlation between the slope of the greyscale calibration curves and the average incident energy.

EXAMPLES

To test the validity of the model we have compared predicted results with measured results for several examples. Figure 4 shows a comparison between a real and simulated image of an aluminum step wedge. This is a single frame image corresponding to an exposure time of 1/30 second. The statistical fluctuations in the number of X-rays striking the image intensifier are obvious in these images, and there is good agreement between real and simulated images. Images resulting from averaging 30 frames are displayed in Fig. 5. Here the reduction in statistical fluctuations is obvious, but agreement between real and simulated images does not appear as good. This is particularly clear in a comparison of the profiles of the two images where the fluctuations are larger for the real image. However, this is understood to be due to pixel-to-pixel variations in the gain of the CCD camera which have not been included in the model.

A test of the performance of the model for thicker materials is presented in Fig. 6 where we show real and simulated images of an iron casting. These images cover an area approximately 10 cm on a side, and the thickness of the casting ranges from 5 mm to 30 mm. Here some of the deficiencies of the model become apparent. Much of the blurring of the edges in the real image is due to scattering which is not properly accounted for in the model. The real image also shows an undercut or brightening around the hole in the casting that is not reproduced in the simulated image. In this case the phosphor bloom is not being properly modeled. In the region of the hole the CCD camera has saturated while the light intensity of the output phosphor has not. Therefore, our model of the phosphor bloom, which is based only on the CCD output level, will not properly mimic the spread of the light in the output phosphor screen. To handle this correctly we will need to treat the image intensifier response and the CCD camera response separately.

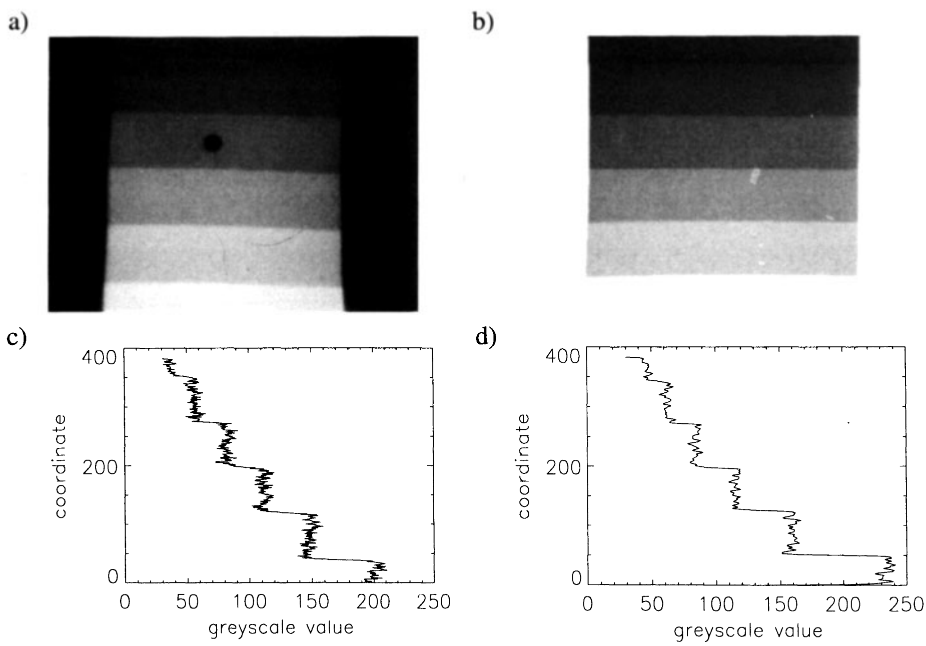

Fig. 4. a) Real, and b) simulated single-frame images of an aluminum step wedge varying in thickness from 5 mm to 20 mm in 3 mm steps. Profiles through the real, and simulated, image are shown in c), and d), respectively.

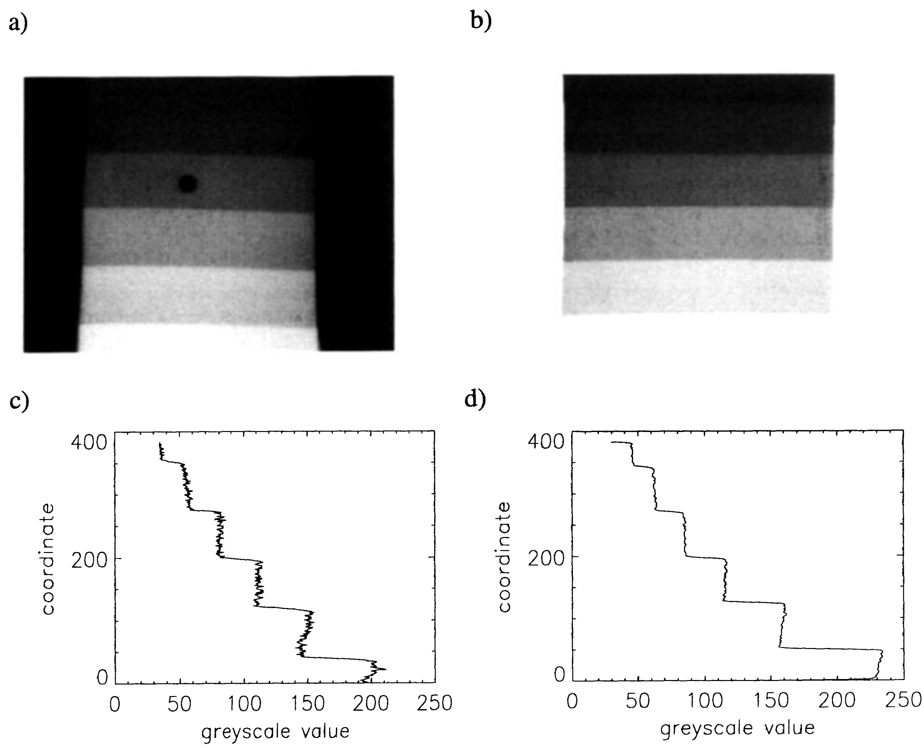

Fig. 5. As in Fig. 4, but averaging over 30 frames.

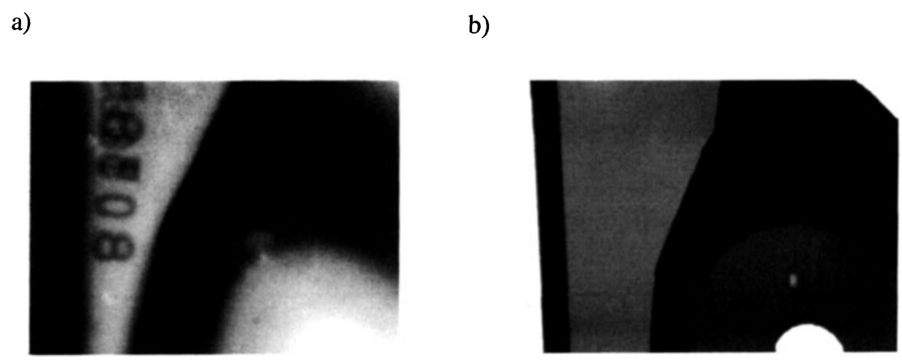

Fig. 6. a) Real, and b) simulated images of an iron casting. The simulated image contains a simulated ellipsoidal flaw located in the thin region above the hole.

CONCLUSIONS

The RTSIM program shows good potential as a tool for evaluating real-time X-ray inspection procedures. The ability to adjust a wide variety of input parameters makes it possible to easily optimize an inspection problem. RTSIM can also provide valuable feedback to a design engineer, allowing consideration of inspectability to influence the design cycle at an early stage. This program has been developed on a DECstation 5000, and should be easily ported to other workstations which run the UNIX operating system and which have C and FORTRAN 77 compilers. Approximately 15 minutes execution time was required to produce the images in the above examples

Work continues on addressing the known limitations of the model. The most important issues to be addressed are proper handling of the undercut and scattering in the sample. We intend to extend the model to handle other CAD formats, and plan to implement a Windows based users interface. Also, it should be straight forward to model the response of a scintillating screen viewed by a CCD camera.

ACKNOWLEDGMENT

This material is based on work sponsored by NIST under cooperative agreement #70NANB9H0916.

REFERENCES

1. Jiadong Xu et al., "Recent Developments in the X-Ray Radiography Simulation Code: XRSIM", *Review of Progress in Quantitative Nondestructive Evaluation* Vol. 13, 557, eds. D.O. Thompson and D.E. Chimenti, Plenum Press, New York (1994).
2. F. Inanc and J. Gray, "New Developments in the Computer Simulation of X-Ray Nondestructive Evaluation Process", *Review of Progress in Quantitative Nondestructive Evaluation* Vol. 10, 355, eds. D.O. Thompson and D.E. Chimenti, Plenum Press, New York (1991).
3. F. Inanc and J. Gray, "A CAD Interfaced Simulation Tool for X-Ray NDE Studies", *Review of Progress in Quantitative Nondestructive Evaluation* Vol. 9, 391, eds. D.O. Thompson and D.E. Chimenti, Plenum Press, New York (1990).
4. J.N. Gray, F. Inanc, and B.E. Shull, "Three Dimensional Modeling of Projection Radiography", *Review of Progress in Quantitative Nondestructive Evaluation* Vol. 8, 345, eds. D.O. Thompson and D.E. Chimenti, Plenum Press, New York (1989).
5. I.P. Csorba, *Image Tubes*, Howard W. Sams & Co., Inc., Indianapolis (1985).
6. S. Kakumanu and J. Gray, "Development of a Model for the X-Ray II-Camera Imaging System and Examples of its Use", *Review of Progress in Quantitative Nondestructive Evaluation* Vol. 13, 685, eds. D.O. Thompson and D.E. Chimenti, Plenum Press, New York (1994).
7. Vivekanand Kini and Joe Gray, "Real Time X-Ray Radiography and its Use in Economic and Fast Tomographic Inspection", *Review of Progress in Quantitative Nondestructive Evaluation* Vol. 13, 541, eds. D.O. Thompson and D.E. Chimenti, Plenum Press, New York (1994).